

Onset of three-dimensional Ir islands on a graphene/Ir(111) template

Peter J. Feibelman

Sandia National Laboratories, Albuquerque, New Mexico 87185-1415, USA

(Received 29 May 2009; published 11 August 2009)

In agreement with observation, local-density approximation (LDA) optimization of one- and two-layer clusters of Ir atoms, adsorbed periodically on a graphene/Ir(111) moiré, shows that the two-layer clusters only become favorable energetically once the clusters comprise as many as 26 adatoms. Heretofore it was known that the LDA predicts smaller islands to grow flat. In showing that the LDA captures the transition to three dimensionality, the present results support its use broadly to analyze Ir island formation on the graphene-covered metal.

DOI: [10.1103/PhysRevB.80.085412](https://doi.org/10.1103/PhysRevB.80.085412)

PACS number(s): 68.43.Bc, 68.43.Fg, 68.43.Hn, 61.46.-w

I. INTRODUCTION

At the lowest coverages, Ir deposited on a graphene/Ir(111) moiré “template” assembles into a well-ordered array of two-dimensional (2D) virtually monodisperse islands.¹ The islands form in regions of the moiré where C atoms lie alternately atop surface Ir atoms, or in fcc hollows. In a recent article, I attributed this phenomenon to a local rehybridization of C-C bonds from the graphene to a local *diamondlike* arrangement.² Where islands form, every other C atom is either displaced down and binds to the surface Ir atom below it, or up, where it binds to an Ir adatom directly above. This picture was drawn from density-functional theory³ (DFT) total-energy calculations in the local-density approximation (LDA).⁴

Preceding this success, as also reported in Ref. 2, similar geometry optimizations had been performed using the Perdew-Wang '91 implementation (PW91) of the generalized gradient approximation (GGA).⁵ The GGA results, however, had failed to agree with the experimental observation that small Ir islands are flat, not three dimensional, and specifically that islands comprising four Ir atoms form a rhombus above the graphene, not a tetrahedron.

The difference in the predicted cluster geometries means that the relative strength of the Ir-C vs the Ir-Ir attraction is larger if one uses the LDA functional⁶ rather than the PW91-GGA. The LDA rhombus “wets” the graphene because in the “LDA universe,” the benefit from forming more Ir-C bonds outweighs the loss incurred by replacing the six Ir-Ir bonds of a pyramidal cluster with only five in a flat island. In the PW91-GGA, such is apparently not the case.

This distinction suggests that until a more universally reliable functional is developed, the LDA is the approximation of choice for the Ir-C system. But, before accepting that suggestion, it is important to check that the LDA ratio of Ir-C to Ir-Ir bond strengths is not *too* strong. That is, granting its correct prediction that small cluster will be flat, it remains important to know if the LDA *also* predicts the island size at which Ir islands first become three dimensional.

The (observed) transition to three dimensionality, as Ir adatoms are added to the islands on the graphene layer, is expected for two reasons. One is that the number of Ir-Ir bonds grows faster with the number of Ir atoms in a compact three-dimensional (3D) as against a 2D cluster. The other is

that as a 2D island grows, it eventually must encroach into graphene regions where C atoms no longer lie atop substrate Ir atoms and where buckling to a diamondlike structure thus becomes less energetically advantageous. At issue, accordingly, is whether the Ir-C interaction in the LDA is so strong that even such encroachment is insufficient to stop the expansion of two-dimensional Ir islands.

N'Diaye *et al.*¹ reported that the transition to three dimensionality, defined as the size at which the numbers of two-dimensional and three-dimensional islands become roughly equal, occurs when the Ir islands comprise about 25 Ir atoms. In this paper, by means of computations for representative islands, I show LDA adsorption energies in substantial agreement with this experimental finding. Specifically, for 26-atom Ir islands, three-dimensional 7 on 19-atom (“magic-on-magic”) clusters first become more strongly bound than two-dimensional flat ones. Thus, the relative strength of Ir-C vs Ir-Ir interactions in the LDA is not unphysically large but quite reasonable.

II. DFT CALCULATIONS

In parallel with Refs. 1 and 2, the energy optimizations reported here were performed using the VASP DFT code^{7,8} with electron-core interactions treated in the projector augmented wave approximation.^{9,10} The focus of the present work, however, is entirely on the results obtained when electron exchange and correlation are represented by the Ceperley-Alder version of the LDA (or CA-LDA).⁶

As in Ref. 2, the present calculations pertain to Ir clusters periodically arrayed on a single graphene layer adsorbed on the upper surface of a four-layer thick Ir(111) slab. Experimentally, graphene is not strictly commensurate with Ir(111), but a 10×10 graphene adlayer on a 9×9 Ir(111) slab is a reasonable model for the observed moiré cell, which accommodates 87 ± 3 Ir atoms.¹

Also following Ref. 2, the present results correspond to a VASP plane-wave basis cutoff of 400 eV and Ir-Ir spacings in the bottom layer of the Ir slab fixed at the LDA bulk value of 2.701 Å. (The experimental room-temperature Ir-Ir nearest-neighbor spacing is 2.715 Å.) The positions of the remaining atoms were allowed to relax until none experienced a force of magnitude of >45 meV/Å. I accelerated electronic relaxation with Methfessel-Paxton Fermi-level smearing

(width=0.2 eV) (Ref. 11) and corrected for the unphysical contact-potential difference associated with having the graphene adlayer on only one side of the Ir slab.¹²

Despite the large, Ir(111) 9×9 , moiré unit cell, the ~ 20 eV width of the occupied $2s-2p$ bands of graphene makes the convergence of surface Brillouin-zone (SBZ) sampling a concern. Based on comparisons reported in Ref. 2, however, an equally spaced 3×3 SBZ sample, including the point $\bar{\Gamma}$, was judged sufficient and used to obtain all the results reported herein.

Ir cluster formation energies cited below are referenced to the cohesive energy of CA-LDA bulk Ir, amounting to 9.4 eV/gas-phase spin-polarized Ir atom. This value, as is typical of the systematic error in LDA calculations, exceeds the 6.9 eV experimental result by 36%. For the sake of comparing two- and three-dimensional cluster energies on the graphene/Ir(111) substrate, this large error is not the main issue. What counts is the relative strength of Ir-Ir and Ir-C bonds, which, in effect, is the subject of the present study.

III. LDA ENERGETICS OF TWO-DIMENSIONAL ISLANDS

To this point the discussion of numerical methods has been standard. The remaining issue is not, namely, deciding what island configurations should be compared, to estimate the number of Ir adatoms, N , at which three-dimensional island formation is first favored. Given a large moiré unit cell, containing 324 Ir slab atoms, 200 C atoms, and N Ir adatoms, and the necessity of sampling the SBZ with a 3×3 mesh of k vectors, each island geometry optimization is time consuming. Thus, to survey many island sizes, shapes, and locations is costly and to be avoided if possible.

To minimize the needed effort, I began by compiling a table of island formation energy versus number of adatoms, N , for 2D Ir islands that are among the best bound by virtue of being localized in the favored hcp region^{1,13} of the graphene-on-Ir(111) moiré and convex, with all corner atoms having three Ir near neighbors.

Earlier results comparing the formation energies of 19-atom two-dimensional islands centered at neighboring sites in the moiré cell yielded a difference of < 0.02 eV/Ir adatom.² For an estimate of when three-dimensional structures become competitive with flat islands, this is an acceptable tolerance. Thus, in the present study I did not survey formation energies as a function of small shifts in island positions.

Table I shows that among the islands I did optimize, as N increased from 1 to 7 to 19, the average chemical potential, $\bar{\mu}$, decreased—as one would expect from the decreasing number of undercoordinated island-perimeter atoms, i.e., from a generalized Gibbs-Thomson relation. The percentage of perimeter atoms continued to decrease when I increased the two-dimensional island size to 26 atoms. Now, however, the chemical potential increased because (cf. Fig. 1) the 26-atom island necessarily encroaches on moiré regions where buckling of the graphene layer to form a local diamond structure is less profitable energetically.

TABLE I. CA-LDA formation energies, $E_{\text{form}}(N)$, and average chemical potentials, $\bar{\mu}$, for the N atom Ir adclusters shown in Fig. 1 as they depend on the numbers of Ir adatoms in the cluster. Note that from the 19- to the 26-atom cluster, the percentage of atoms on the perimeter diminishes, but the chemical potential increases.

N	Perimeter atoms (%)	$E_{\text{form}}(N)$ (eV)	$\bar{\mu}$ (eV)	Definition of $\bar{\mu}$
1	100	4.72	4.72	$E_{\text{form}}(1)$
7	86	2.75	2.42	$[7E_{\text{form}}(7) - E_{\text{form}}(1)]/6$
19	63	1.97	1.49	$[19E_{\text{form}}(19) - 7E_{\text{form}}(7)]/12$
26	58	1.92	1.78	$[26E_{\text{form}}(26) - 19E_{\text{form}}(19)]/7$

The $N=26$ island is a reasonable stopping point for optimizations of two-dimensional islands both because the encroachment argument implies that at larger N the chemical potential will only increase further and because it allows for an energy comparison with the smallest magic-on-magic (i.e., 7-atom regular hexagonal on 19-atom regular hexagonal) three-dimensional example. This comparison, as detailed below, favors the three-dimensional island, whereas several comparisons of two- and three-dimensional islands for smaller N all favor two dimensionality. This discussion is the basis for concluding that in the LDA universe, the transition to three dimensionality occurs at $N \approx 26$, in good agreement with the observations reported in Ref. 1.

Of interest relative to the discussion in Sec. IV, the optimized two-dimensional islands of Fig. 1 are rather flat. The maximum Ir adatom height differences in the 7-, 19-, and

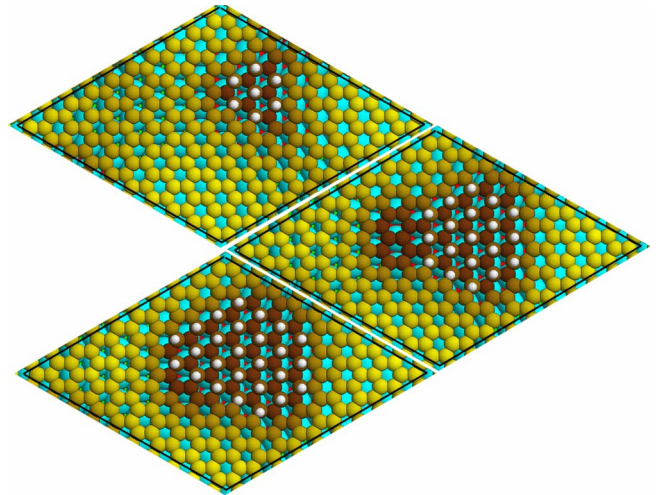


FIG. 1. (Color online) Two-dimensional islands containing 7-, 19-, and 26-Ir adatoms on the graphene-on-Ir(111) substrate. The Ir atoms of the first, second, and third metal layers are colored cyan, red, and green. The colors of the C atoms are brown (for the lowest, lying a little more than 2 Å above the Ir surface layer) to yellow (for the highest, lying about 1.9 Å higher). The spheres representing Ir adatoms are white, with sizes reduced to allow a view of where the adatoms reside. Thus, one can see that the islands of all three panels are adsorbed in the hcp region of the moiré, where red second-layer Ir atoms are visible through the C-atom hexagons (cf. Ref. 13). The black lines in each panel delimit the moiré unit cell.

TABLE II. CA-LDA formation energies, $E_{\text{form}}(N)$, for the N atom Ir adclusters schematized in Figs. 1 and 2 as they depend on the numbers of Ir adatoms in the first- and second-cluster layers. If the latter is zero, the cluster is two dimensional. For each N , the formation energy of the preferred cluster geometry is printed in boldface.

N	Layer 1	Layer 2	No. of Ir-Ir bonds	No. of Ir-Ir bonds/ N	$E_{\text{form}}(N)$ (eV)
19	19	0	42	2.21	1.97
19	12	7	45	2.37	2.10
21	21	0	47	2.24	1.98
21	14	7	62	2.95	2.07
26	26	0	60	2.31	1.92
26	16	10	83	3.19	1.90
26	19	7	75	2.88	1.89

26-atom islands are 0.08, 0.06, and 0.17 Å. Moreover, the larger height difference for the 26-atom island is attributable to the curvature of the underlying graphene layer. The conclusion is that the Ir adatoms' preference is to accommodate the difference between the C-C repeat distance on the Ir(111) surface of ~ 2.44 Å and the 2.70 Å Ir-Ir nearest-neighbor distance in the bulk metal rather than to buckle and thereby improve the Ir-Ir binding. This result, expressing a preference for "wetting," has two likely sources. One is that the "natural" Ir-Ir distance should be shorter when the Ir atoms are undercoordinated, i.e., with three to six Ir neighbors as against 12 in the fcc metal. The other is the strong Ir-C bonding.

IV. LDA ENERGETICS OF THREE-DIMENSIONAL ISLANDS

In this section, I compare the formation energies of two- and three-dimensional Ir islands containing 19, 21, and 26 adatoms. In each case, the main issues are whether the Ir-Ir bonds are strong and numerous enough to favor three dimensionality and, as a corollary, what the preferred island structures are.

Table II summarizes the results, which show a preference for three-dimensional islands once $N=26$ and the largest preference for the nominally magic-on-magic case of a 7-atom regular hexagonal second-layer island residing on a 19-atom regular hexagonal first-layer cluster. In this case, the three-dimensional island is favored by 0.03 eV/Ir atom, in accord with the experimental observation of roughly equal numbers of two- and three-dimensional islands at $N \approx 25$, after growth at 350 K ($=0.031$ eV).

Figure 2, showing the geometry of the best 26-Ir cluster, among others, makes clear that "magic on magic" considerably overstates the perfection of its hexagon on hexagon arrangement. Indeed, all the optimized two-layer clusters shown are buckled. This result, in contrast to the two-dimensional islands (cf. Sec. III), manifests the compromise, in each case, between epitaxial match with the underlying graphene layer and maximizing the strength of the Ir-Ir bonds.

Requiring upper and lower layers to have only 120° corners, the smallest two-layer island comprises 19 Ir adatoms,

as shown in Fig. 2(a). In this example, the central atom of the upper layer lies some 0.9 Å higher than the average of its six intraplanar neighbors. The next bigger two-layer island with 120° corners is shown in Fig. 2(b). Note that both its lower and upper layers are buckled. From the energetic perspective, as seen in Table II, the extension of the lower layer has added enough structural flexibility that, compared to the smaller island, the island formation energy has dropped by 0.03 eV/Ir atom, making it more competitive with an $N=21$ flat island.

This trend persists in the 26-atom cases studied. Now, there are two distinct two-layer geometries with only 120° corners, the magic-on-magic case shown in Fig. 2(c) and the

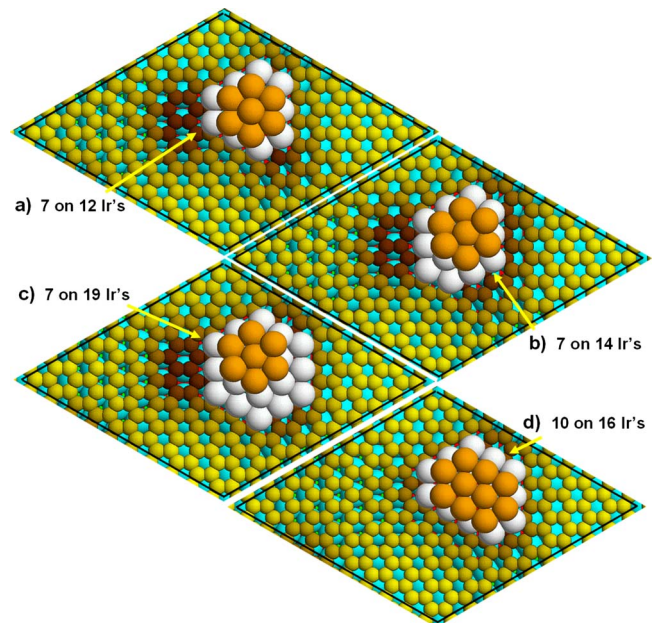


FIG. 2. (Color online) Three-dimensional islands containing 19-, 21-, and 26-Ir adatoms on the graphene-on-Ir(111) substrate. The Ir adatoms of the first, second, and third metal layers are colored cyan, red, and green. The colors of the C atoms are brown (for the lowest lying) to yellow (the highest). The clusters' first-layer Ir adatoms are white and their second-layer atoms are orange. The black lines in each panel delimit the moiré unit cell.

“10 on 16 Ir” example shown in Fig. 2(d). For the main purpose of the present work, what is important is that both species of three-dimensional 26-atom islands have lower formation energy than the 2D 26-atom case. For the sake of interpretation, it is also of interest that the island shown in Fig. 2(c), which has fewer Ir-Ir and more Ir-C bonds, is the better bound. This is likely because, as the figures reveal, it has more freedom to warp.

V. DISCUSSION

The results presented here suggest using the CA-LDA for follow-up studies of the *growth* of cluster arrays on a graphene-covered Ir(111) surface. The highest priority investigations will address the kinetics of cluster formation.¹⁴ One issue is how Ir adatoms and dimers diffuse over the graphene moiré. Another is the nature of the transition from two to three dimensionality. Neither preliminary calculation nor experiment favors the idea that 3D clusters form as a result of the trapping of second-layer Ir adatoms on top of one-layer islands. The calculations show that a second-layer Ir adatom gains a minimum of 0.56 eV by moving off the first layer of

a 19-atom flat island into a site adjacent to it. The Ehrlich-Schwoebel barrier^{15,16} to this process is unlikely to be large.¹⁷ Thus 3D island formation must involve some sort of collective dewetting transition.

Apart from studies of growth kinetics, further confirmation of the accuracy of the CA-LDA might be provided by high-resolution structural observations of individual clusters using scanning tunneling microscopy. Studies involving other metal substrates and adatom species would be desirable toward potential catalytic and magnetic applications of the ordered arrays. Recent calculations of atomic H on graphene suggest that buckling and rehybridization represent a quite general adsorption mechanism.^{18,19}

ACKNOWLEDGMENTS

This work was supported by the Office of Basic Energy Sciences, Division of Materials Science and Engineering, DOE. Sandia is operated by the Lockheed Martin Co. for the National Nuclear Security Administration, U.S. Department of Energy under Contract No. DE-AC04-94AL85000. vASP was developed at T. U. Wien’s Institut für Theoretische Physik.

-
- ¹A. T. N’Diaye, S. Bleikamp, P. J. Feibelman, and T. Michely, *Phys. Rev. Lett.* **97**, 215501 (2006).
²P. J. Feibelman, *Phys. Rev. B* **77**, 165419 (2008).
³P. Hohenberg and W. Kohn, *Phys. Rev.* **136**, B864 (1964).
⁴W. Kohn and L. J. Sham, *Phys. Rev.* **140**, A1133 (1965).
⁵J. P. Perdew, in *Electronic Structure of Solids ‘91*, edited by P. Ziesche and H. Eschrig (Akademie Verlag, Berlin, 1991); J. P. Perdew, J. A. Chevary, S. H. Vosko, K. A. Jackson, M. R. Pederson, D. J. Singh, and C. Fiolhais, *Phys. Rev. B* **46**, 6671 (1992); **48**, 4978 (1993).
⁶D. M. Ceperley and B. J. Alder, *Phys. Rev. Lett.* **45**, 566 (1980); as parametrized by J. P. Perdew and A. Zunger, *Phys. Rev. B* **23**, 5048 (1981).
⁷G. Kresse and J. Hafner, *Phys. Rev. B* **47**, 558 (1993); **49**, 14251 (1994).
⁸G. Kresse and J. Furthmüller, *Comput. Mater. Sci.* **6**, 15 (1996); *Phys. Rev. B* **54**, 11169 (1996).
⁹P. E. Blöchl, *Phys. Rev. B* **50**, 17953 (1994).
¹⁰G. Kresse and D. Joubert, *Phys. Rev. B* **59**, 1758 (1999).
¹¹M. Methfessel and A. T. Paxton, *Phys. Rev. B* **40**, 3616 (1989).
¹²J. Neugebauer and M. Scheffler, *Phys. Rev. B* **46**, 16067 (1992).

- ¹³The “hcp region” of the moiré is where the C atoms reside close to directly atop either a surface layer Ir atom or an fcc threefold hollow. Accordingly, subsurface Ir atoms (colored red in Figs. 1 and 2) can be seen through C-atom hexagons in the hcp region. Similarly, third-layer Ir adatoms (colored green in Figs. 1 and 2) are seen through C-atom hexagons in the “fcc region” of the moiré, and surface Ir adatoms are visible through the C-atom hexagons in the “atop region.” According to Ref. 1, Ir islands on graphene/Ir(111) equilibrate in the hcp region of the moiré.
¹⁴For a perspective on kinetically driven transitions from 2D to 3D island growth in homoepitaxy, see, e.g., J. Tersoff, A. W. Denier van der Gon, and R. M. Tromp, *Phys. Rev. Lett.* **72**, 266 (1994).
¹⁵R. L. Schwoebel and E. J. Shipsey, *J. Appl. Phys.* **37**, 3682 (1966).
¹⁶G. Ehrlich and F. G. Hudda, *J. Chem. Phys.* **44**, 1039 (1966).
¹⁷T. T. Tsong, *Prog. Surf. Sci.* **64**, 199 (2000), Table II quotes an excess barrier, relative to terrace diffusion, of about 0.2 eV to descend a step on pure Ir(111).
¹⁸Y. Lin, F. Ding, and B. I. Yakobson, *Phys. Rev. B* **78**, 041402 (2008).
¹⁹A. K. Singh and B. I. Yakobson, *Nano Lett.* **9**, 1540 (2009).